

Diffraction in Deep Inelastic Scattering: the hadronic nature of Quarks

L. Dick, CERN, Geneva, Switzerland

V. Karapetian, CERN, Geneva, Switzerland

R. Barni, Dip. di Fisica, Univ. degli Studi, and INFN, Sezione di Milano, via Celoria, 16 I-20133 Milano, Italy

G. Preparata, Dip. di Fisica, Univ. degli Studi, and INFN, Sezione di Milano, via Celoria, 16 I-20133 Milano, Italy

Abstract

We analyse the “diffractive” events reported by the HERA groups within a theoretical framework (Anisotropic Chromo Dynamics, ACD) that attributes to the fundamental quanta of QCD (Quarks and Gluons) a completely hadronic behaviour except, of course, for the Quark “point-like” coupling to the electroweak fields.

The remarkable success of our calculation, free of adjustable parameters, highlights the fallacy of considering “short-distance” physics as autonomous (indeed orthogonal) from the long-distance, colour confining hadronic physics.

arXiv:hep-ph/9608217v1 2 Aug 1996

1 Introduction

One of the most relevant and surprising aspects of the physics produced by HERA in the last four years is the discovery of a large number of events whose final states are characterised by large rapidity gaps [1], of the kind one observes in diffractive events in purely hadronic interactions [2]. This occurrence is all the more surprising since “Diffraction”, or in general the physics of the Pomeron, is considered to be the genuine manifestation of the dynamics of QCD at large distances, or at small transverse momenta, where perturbation theory (PQCD) has absolutely nothing to say, the main actors being the Hadrons, the permanent prisons of Quarks and Gluons. On the other hand Deep Inelastic Scattering (DIS) is generally considered the true realm of QCD at short space-time distances where Asymptotic Freedom (AF) should allow us, should it not?, to compute the basic inclusive cross-section through the simple Feynman rules of PQCD.

In hindsight a number of PQCD mechanisms [3, 4] have been invoked in order to save the general expectations based on AF, but the puzzle that stands in the way of the natural philosopher is to understand why a typical hadronic behaviour, completely extraneous to PQCD, can indeed be mimicked in a world thoroughly governed by this simple (unconfined) realization of QCD.

Almost a quarter of a century ago one of us (G.P.) found that the fundamental aspects of the just discovered Bjorken scaling behaviour could be easily and naturally accounted for by assuming that Quarks (and later Gluons) would behave at any space-time scale like hadronic particles [5], with their Regge behaviours that were known since long to well describe high energy interactions [6]. Naturally in the Massive Quark Model (MQM) [5] no attempt was made to derive “Reggeism” from any basic Lagrangian, the only firm Ansatz being that Regge behaviour, and in particular the Pomeron and Diffraction, should be properties of the Quarks as well. It should be perfectly clear that such an attitude was then (and is now) completely at variance with the beliefs and the expectations of the vast majority of the particle physicists; however it is a fact that the recent observations at HERA do agree with those distant attempts, while they have posed and continue to pose some non-trivial problems to the theorists of PQCD.

While along the paths indicated by AF PQCD has developed into an extremely powerful and flexible means to deal with DIS physics, the MQM has gone through the much more uncertain steps that have led it to Anisotropic Chromo Dynamics (ACD) [7], the “effective” Lagrangian which governs the dynamics of QCD over a peculiar confining vacuum (the Chromo Magnetic Liquid, CML [8]) that has definite chances to well approximate the true QCD vacuum. Recently one has been able to find within ACD a simple and satisfactory approach to the Pomeron and Diffraction [9] that embodies in a physically transparent way the pioneering approach of Low and Nussinov [10].

2 Diffractive Deep Inelastic Scattering

The basic idea is that when the Quarks of two Hadrons collide at high energy (see Fig.1) and interact by the fundamental colour-exchange potential, the Hadrons (the colour-singlets) of the final state comprise two different (in our case) $Q\bar{Q}$ -pairs whose masses are of the order of the CM energies, which then fill the final states with the products of their decay [11]. A detailed calculation [9] shows that the diagrams in Fig.1 correctly reproduce the main characteristic of the Pomeron. As for single Diffraction in DIS the relevant diagrams are reported in Fig.2, where it should be noticed that the deep inelastic photon couples to the Quarks through a “point-like wave function”.

The virtual photon-proton diffractive cross section is given by a tedious but straightforward calculation of the Feynman-like diagrams of Fig.2, whose only “unorthodox” elements are:

- (i) the proton wave-function that projects the initial hadronic state (the proton) onto its constituent quark state which in the high energy limit ($W_{\gamma^*p} \rightarrow \infty, x_{Bj} \rightarrow 0$) can be taken as:

$$|\vec{p}\rangle = \int d^3\vec{p}_1 d^3\vec{p}_2 \sqrt{\frac{(2\pi)^3 2E_p}{(2\pi)^9 2E_1 2E_2 2E_3}} \phi(\vec{p}_1, \vec{p}_2) |\vec{p}_1, \vec{p}_2, \vec{p} - \vec{p}_1 - \vec{p}_2\rangle \quad (1)$$

with the normalisation

$$\int d^3\vec{p}_1 d^3\vec{p}_2 |\phi(\vec{p}_1, \vec{p}_2)|^2 = 1, \quad (2)$$

and the factorisation property ($\vec{p}_i = x_i\vec{p} + \vec{p}_{\perp i}$), $|\vec{p}_{\perp i}| \ll |\vec{p}|$

$$\phi = \phi_L(x_1, x_2) \cdot \phi_T(\vec{p}_{\perp 1}, \vec{p}_{\perp 2}), \quad (3)$$

which allows the complete separation of the trivial longitudinal dynamics from the transverse one. We parameterise $\phi_T(\vec{p}_{\perp 1}, \vec{p}_{\perp 2})$ as a Gaussian distribution [9]

$$\phi_T(\vec{p}_{\perp 1}, \vec{p}_{\perp 2}) = \sqrt{12} \frac{b}{\pi} \exp[-b(p_{\perp 1}^2 + p_{\perp 2}^2 + (\vec{p}_{\perp 1} + \vec{p}_{\perp 2})^2)] \quad (4)$$

with $b = 17 \text{ GeV}^{-2}$, as determined by the slope of the forward peak in the pp elastic cross section.

- (ii) the diffractive final state comprises two Fire String (FS) states [11], whose decay products are the Hadrons of the final states. Please note that in the inclusive cross-section Quark-Hadron “duality” [13] allows us to integrate over the quark degrees of freedom only;
- (iii) the ACD gluon propagator [7], whose form can be taken as:

$$G_{\mu\nu}^{ab}(q) = \delta^{ab} g_{\mu\nu} 8\pi\mu^2 \frac{3\alpha^2 - |q^2|}{(\alpha^2 + |q^2|)^3} = \delta^{ab} g_{\mu\nu} 8\pi\mu^2 V(q^2), \quad (5)$$

giving rise to an interquark effective potential $\tilde{V}(r) = \mu^2 r e^{-\alpha r}$, where the two parameters μ , the effective string tension, and the “longitudinal size” of the “chromomagnetic needle” α^{-1} , are fixed by the analysis of the hadronic spectrum [14] as (m_g denotes the gluon mass)

$$\mu = 0.475 \text{ GeV}, \quad \alpha = 2\sqrt{2}m_g = 0.40 \text{ GeV}. \quad (6)$$

The result of the calculation can be expressed in terms of a diffractive structure function F_2^D :

$$\left. \frac{d\sigma^{\gamma^* p \rightarrow Xp}}{d\eta_{\mathbb{P}} dt} \right|_{diff} = \frac{4\pi^2 \alpha_{QED}}{Q^2(1-x_{Bj})} \frac{dF_2^D}{d\eta_{\mathbb{P}} dt}(x_{Bj}, Q^2, \eta_{\mathbb{P}}, t) \quad (7)$$

$$\eta_{\mathbb{P}} = \frac{M_X^2 + Q^2 - t}{W^2 + Q^2 - M_p^2} = \frac{x_{Bj}}{\beta} \sim 1 - x_F, \quad \beta = \frac{Q^2}{M_X^2 + Q^2 - t} \quad (8)$$

where (x_F is the Feynman variable of the final state proton, M_X is the invariant hadronic mass, t is the invariant momentum transferred to the final state proton). F_2^D is given by the expression

$$\frac{dF_2^D}{d\eta_{\mathbb{P}} dt} = \frac{N}{\eta_{\mathbb{P}}} I(t)^2 J(x_{Bj}, Q^2)(1-x_{Bj}), \quad (9)$$

where the normalisation contains the couplings, the colour factor, the sum over active quark flavour and the other numerical factors,

$$N = \sum_f Q_f^2 \mathcal{C}_F \cdot \left(\frac{\mu}{\alpha}\right)^{12} \cdot \frac{96}{\pi^9 \alpha^2} \sim 1.77 \cdot 10^{-2} \text{ GeV}^{-2} \quad (10)$$

$$I(t) = \int d^2\vec{w} V(\vec{w} - \vec{x}_0) V(\vec{w} + \vec{x}_0) (e^{-\delta x_0^2} - e^{-\delta w^2}) \quad (11)$$

with $\vec{x}_0 = \frac{\vec{p}_{\perp}}{2\alpha}$ the transverse momentum of the final state proton, and $\delta = b\alpha^2 \simeq 3$. Furthermore

$$J(x, Q^2) = \int d^2\vec{\xi} d^2\vec{z} z^2 \ln \frac{W_{\gamma^* p}^2}{z^2} V(\vec{z})^2 [\phi_{\gamma}(\vec{\xi}, 0) - \phi_{\gamma}(\vec{\xi}, \vec{z})] \quad (12)$$

where the “photon wave-function” $\phi_\gamma(\vec{\xi}, \vec{z})$ is given by ($A = \frac{Q^2}{\alpha^2}$):

$$\phi_\gamma(\vec{\xi}, \vec{z}) = \int_0^1 d\tau \frac{\tau^2 \vec{\xi} \cdot (\vec{\xi} + \vec{z}) A}{[\tau(1-\tau)A + \vec{\xi}^2][\tau(1-\tau)A + (\vec{\xi} + \vec{z})^2]}. \quad (13)$$

A few observations on Eqs. (5) to (9) are in order:

- (a) the energy dependence is logarithmic, thus no “unitarization” is necessary to obey the Froissart bound [15];
- (b) in the limited kinematic range now accessible to the experiments such logarithmic behaviour can well mimic a power law, which is favoured by the experimental fits;
- (c) the factorisation of the diffractive structure function as

$$F_2^D(\eta_{\mathbb{P}}, \beta, Q^2) \sim \Phi(\eta_{\mathbb{P}}) \cdot F_2^{\mathbb{P}}(\beta, Q^2) \quad (14)$$

is broken due to the t -integration of equation (11) and to the contribution of diagrams subleading respect to that of Fig. 2, however, as one can see from Fig. 3, in the experimentally accessible region our result is effectively factorized; with factorizable form the $F_2^{\mathbb{P}}(\beta, Q^2)$ can be associated with Pomeron structure function, as it is discussed in the pioneer work [16].

- (d) when $\beta \rightarrow 0$, corresponding to very large diffractive masses, the typical HERA energies ($W_{\gamma^*p} \simeq 100$ GeV) imply that $\eta_{\mathbb{P}}$ becomes rather sizeable, thus requiring the introduction of sub-leading Regge trajectories, like ω, f_2, \dots, π , as suggested by purely hadronic data [17, 2], that we have neglected in our calculation. Since such contributions can alter the form of the flux function $\Phi(\eta_{\mathbb{P}})$, the extraction of $F_2^{\mathbb{P}}(\beta, Q^2)$ can be more safely performed by integrating F_2^D in each bin of the (β, Q^2) -plane, rather than fitting the F_2^D -function with a universal power law over a fixed $\eta_{\mathbb{P}}$ interval which is then used in the determination of $F_2^{\mathbb{P}}$, as is commonly done by the HERA Collaborations [18, 19].

3 Comparison with experimental data

Our calculation of the triple differential structure function $F_2^D(\eta_{\mathbb{P}}, \beta, Q^2)$ is compared with the experimental data from the ZEUS Collaboration [18] in Fig. 3 and from the H1 Collaboration [19] in Fig. 4. One notes good agreement with observations for all accessible values of β, Q^2 and $\eta_{\mathbb{P}}$, leading to overall statistical value $\chi^2/\text{d.f.} = 67.4/96$ being compared with data. In order to see the consistency of both H1 and ZEUS data we performed a new power-law fit to the combined set of data (shown in double-log scale in Fig. 3 and Fig. 4 by straight line dependence), which yielded the universal value of the Pomeron intercept $\alpha_{\mathbb{P}}(0) = 1.069 \pm 0.030$ ($\chi^2/\text{d.f.} = 33.33/47$ [H1], $4.05/23$ [ZEUS] assuming full errors in the fit as statistical and systematic errors added in quadrature). Within experimental errors, this value of $\alpha_{\mathbb{P}}(0)$ is consistent with a soft supercritical Pomeron [20] and is correctly reproduced by our model.

Our prediction for double differential structure functions $F_2^D(\beta, Q^2)$ and $F_2^D(x_{Bj}, Q^2)$ is reported for different values of Q^2 in Fig. 5 and compared with data points from both ZEUS and H1 [18, 19, 21]. Again good agreement is to be noted. In particular a smooth Q^2 -dependence is naturally reproduced by the model. To calculate the β -distributions, the underlying $\eta_{\mathbb{P}}$ -integration is performed for two different intervals defined by HERA Collaborations [18, 19], and we find that the discrepancies in the values of the Pomeron structure function measured by H1 and ZEUS does depend on such difference. Indeed, as one can see in Fig. 5, our model favours a small β -dependence in the Pomeron structure function. The present (1993) data are statistically compatible with both the model of Ref. [18] and our predicted flat β -dependence. With more precise data it will certainly be possible to distinguish between the two approaches. But in this case we must be more careful in data analysis because the unfolding procedure (to calculate the acceptance and compensate kinematic cuts effects) based on Monte Carlo simulations [18, 19, 21] can give undesirable correlations between the model

to be tested and the corrected data [18, 19], since β -distribution affects, in particular, the mass spectrum of hadronic final states. Clearly, a better comparison of our model could be made by processing with it the raw data.

Finally, our expectation for the total contribution of Single Diffractive Dissociation (SDD) process is given in the last four pictures in Fig. 5, in terms of scaling variable x_{Bj} and for different values of Q^2 . The relevant upper limit for the η_P -integration must be chosen about 0.15, in accordance with pure hadronic data [17, 2]. Note, that the decrease of F_2^D to zero at $x_{Bj} = 10^{-2}$ is due to the special kinematic and experimental conditions at HERA. When these limitations are removed it is seen that the real contribution of SDD to DIS is closer to 20% than to 10%, as claimed by the HERA groups. This discrepancy is due to their procedure for selecting large rapidity gap events and to the far from ideal acceptance of their setup for diffractive physics.

4 Conclusion

To conclude this letter, we may state with confidence that a sound, realistic and conceptually simple explanation has emerged from ACD of the complex features of Diffraction in DIS discovered by HERA. The main message of this paper, we believe, is the further proof of the correctness of the idea that deep inelastic phenomena fully exhibit the basic features of high energy hadronic dynamics, albeit at the level of the fundamental quarks instead of the composite hadrons. On the other hand the hadronic nature of the quarks that is corroborated by this work is, to our mind, a further stumbling block on the road of PQCD, which looks at the deep inelastic world as completely different and separated (by the scale Λ_{QCD}) from the world of long-distance (low p_T) phenomena. Finally we notice that the same ideas can be employed to compute the non-diffractive low x_{Bj} part of the structure function, which shall be reported in a future publication.

Acknowledgement

One of us (R.B.) is pleased to recognise the help from P. G. Ratcliffe and T. Sanvito in the preliminary stage of the work.

References

- [1] ZEUS Collaboration, M. Derrick et al., Phys. Lett. B315 (1993) 481.
- [2] K. Goulianos, Phys. Reports 101 (1983) 169.
- [3] W. Buchmüller, Phys. Lett. B353 (1995) 335; W. Buchmüller, A. Hebecker, Phys. Lett. B355 (1995) 573.
- [4] N.N. Nikolaev, B.G. Zakharov, JETP 78 (5) (1994) 598; M. Genovese, N.N. Nikolaev, B.G. Zakharov, JETP 81 (4) (1995) 625.
- [5] G. Preparata, Phys. Rev. D7 (1973) 2973; G. Preparata, Nucl.Phys. B80 (1974) 299; G. Preparata, Proceedings of International School of Subnuclear Physics, 'Ettore Majorana', 12th course, Erice, Sicily, 1974.
- [6] P.D. Collins, Introduction to Regge theory, Cambridge University Press, 1977.
- [7] G. Preparata, Phys.Lett. B102 (1981) 327; G. Preparata, Phys.Lett. B108 (1982) 187; J.L. Basdevant, G. Preparata, Il Nuovo Cim. 67A (1982) 19.
- [8] G. Preparata, Nucl. Phys. B201 (1988) 139; G. Preparata, Il Nuovo Cim. 103A (1990) 1073.
- [9] G. Preparata, P.G. Ratcliffe, Phys. Lett. B345 (1995) 272.
- [10] F.E. Low, Phys. Rev. D12 (1975) 163; S. Nussinov, Phys. Rev. Lett. 34 (1975) 1286.
- [11] G. Preparata, G. Valenti, Nucl.Phys. B183 (1981) 50; L. Angelini et al., Comput. Phys. Commun. 67 (1991) 293; L. Angelini et al., Z.Phys. C44 (1989) 599.
- [12] A. H. Mueller, Phys. Rev. D23 (1970) 2963; R.C. Browner et al., Phys. Reports 14 (1974) 260.
- [13] P. Cea, P. Colangelo, G. Nardulli, G. Preparata, Phys. Lett. B115 (1982) 310.
- [14] G. Preparata, M. Scorletti, Phys. Rev. D49 (1994) 5984.
- [15] M. Froissart, Phys. Rev. 123 (1961) 1053; A. Martin, Phys. Rev. 124 (1963) 1432.
- [16] G. Ingelman, P.E. Schlein, Phys. Lett. B152 (1985) 256.
- [17] S. N. Ganguli, D. P. Roy, Phys. Reports 67 (1980) 201.
- [18] ZEUS Collaboration, M. Derrick et al., Z. Phys. C68 (1995) 569;
- [19] H1 Collaboration, T. Ahmed et al., Phys. Lett. B348 (1995) 681.
- [20] A. Donnachie, P.V. Landshoff, Phys. Lett. B296 (1992) 227.
- [21] H1 Collaboration, T. Ahmed et al., DESY 95-006 (1995).

Captions

Fig. 1

The amplitude dominating the total cross-section for meson-meson scattering at high energy (all the diagrams obtained by permutations of the quark-gluon vertices should be summed).

Fig. 2

The amplitude dominating the single diffractive cross-section for DIS at high energy W_{γ^*p} and large diffracted mass M_X^2 (the so called Triple-Regge regime [12]).

Fig. 3

The triple differential structure function F_2^D of ZEUS is compared with our calculation (broken line), first passing through all the experimental cuts (dotted line) and then relaxing the cuts, but in the integration region defined by ZEUS (full line) and with a power-law fit (dashed line). The almost negligible contribution of non-factorisable diagrams is also shown (dot-dashed line). Note that the 15% contribution due to double diffraction has been subtracted from data [18].

Fig. 4

The triple differential structure function F_2^D of H1 is compared with our calculation (broken line), first passing through all the experimental cuts (dotted line) and then relaxing the cuts, but in the integration region defined by H1 (full line) and with a power-law fit (dashed line). Note that the 15% contribution due to double diffraction has been subtracted from data [18].

Fig. 5

The double differential structure function F_2^D of ZEUS and H1 in terms of β and x_{Bj} , predicted by the model (full line) and compared with the experimental data. The black points on β -distribution correspond to $\alpha_P(0) = 1.069$, obtained in our power-law fit to combined set of HERA data. The black and white points on x_{Bj} -distribution are observations using two different analysis methods [21], the vertical lines are pure kinematic cuts. Note that the 15% contribution due to double diffraction has been subtracted from data [18]. The last four pictures show the expected contribution of single diffraction dissociation, integrated with the relaxed upper limit on η_P (see text above).

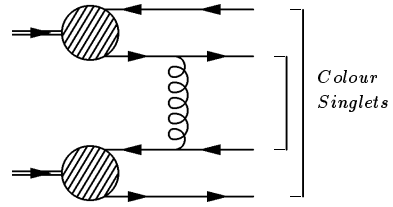


Figure 1: The amplitude dominating the total cross-section for meson-meson scattering at high energy (all the diagrams obtained by permutations of the quark-gluon vertices should be summed).

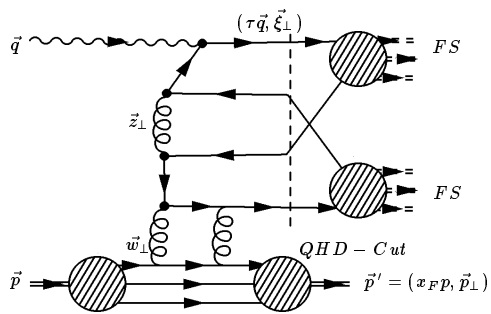


Figure 2: The amplitude dominating the single diffractive cross-section for DIS at high energy W_{γ^*p} and large diffracted mass M_X^2 (the so called Triple-Regge regime [12]).

The Proton Diffractive Structure Function $F_2^D(\eta_P, \beta, Q^2)$: ZEUS Data

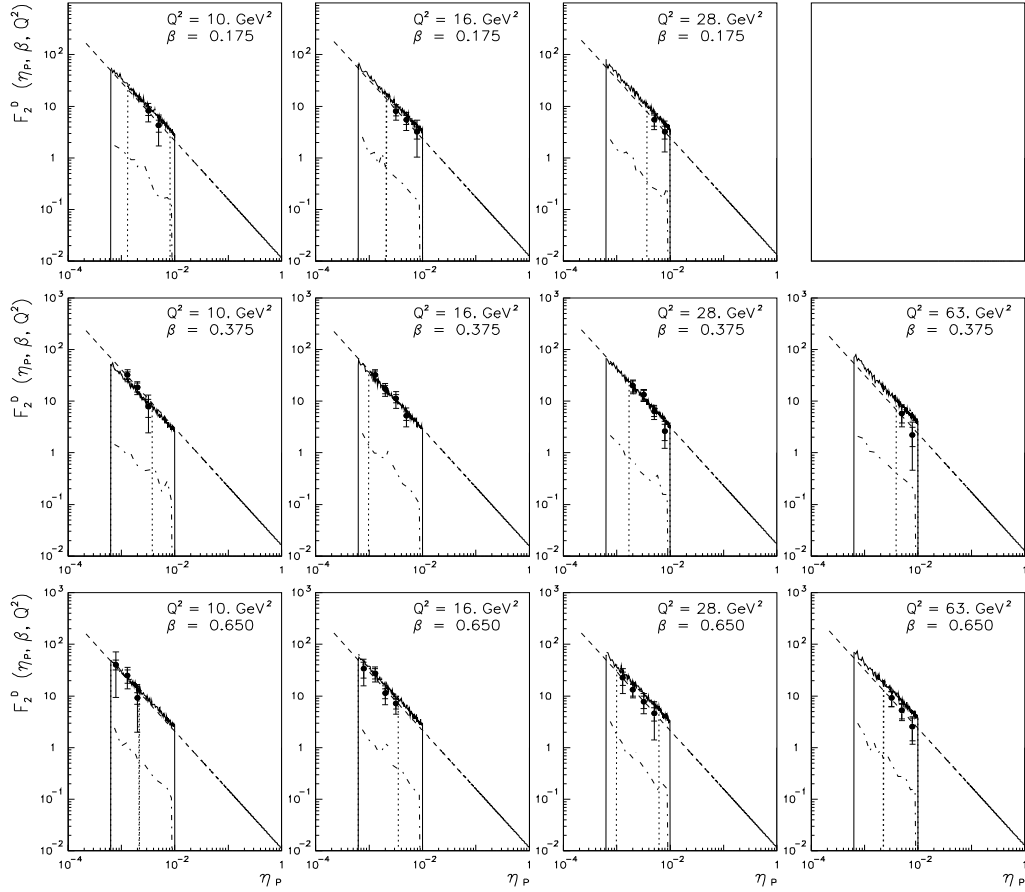


Figure 3: The triple differential structure function F_2^D of ZEUS is compared with our calculation (broken line), first passing through all the experimental cuts (dotted line) and then relaxing the cuts, but in the integration region defined by ZEUS (full line) and with a power-law fit (dashed line). The almost negligible contribution of non-factorisable diagrams is also shown (dot-dashed line). Note that the 15% contribution due to double diffraction has been subtracted from data [18].

The Proton Diffractive Structure Function $F_2^D(\eta_P, \beta, Q^2)$: H1 Data

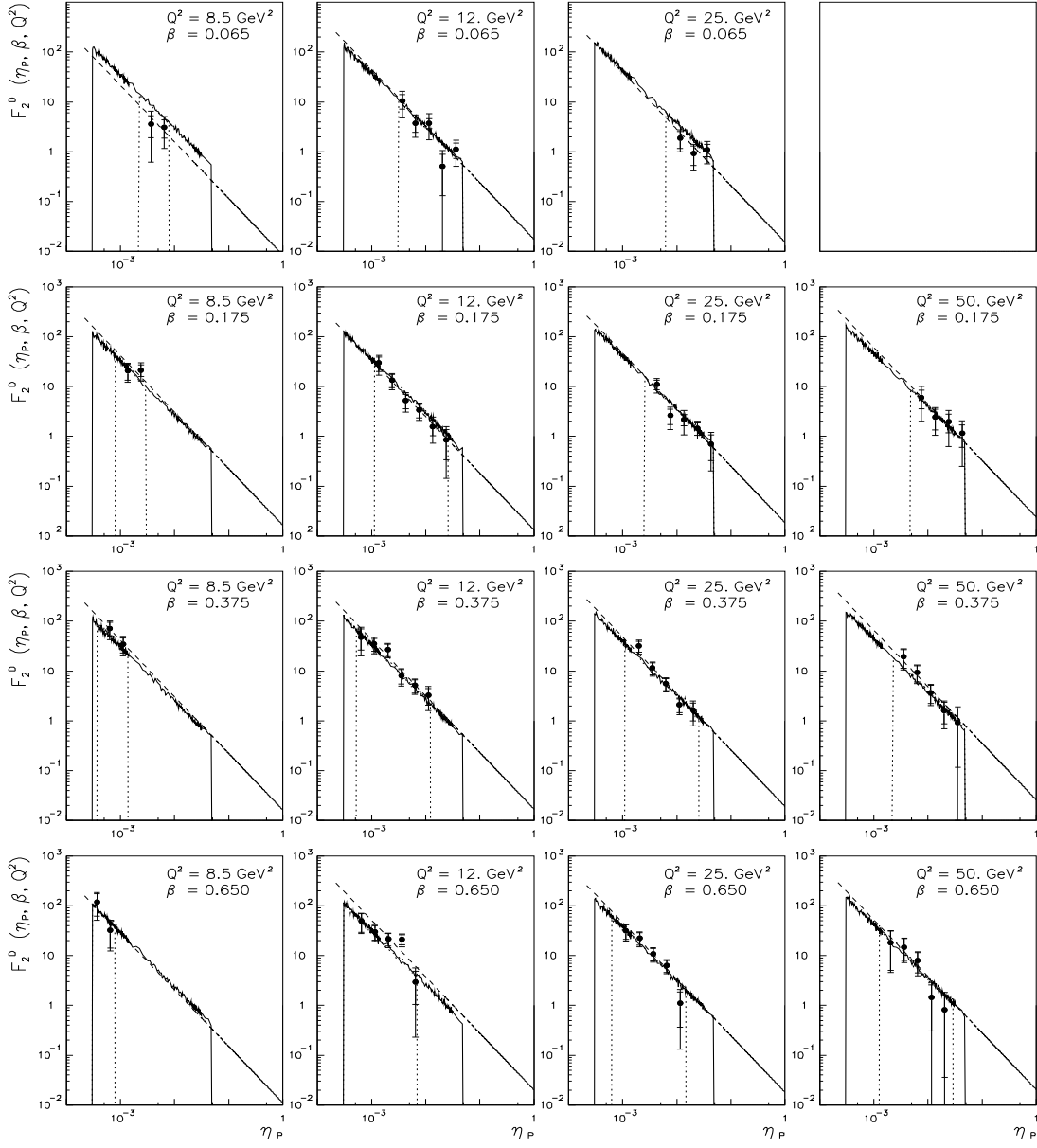


Figure 4: The triple differential structure function F_2^D of H1 is compared with our calculation (broken line), first passing through all the experimental cuts (dotted line) and then relaxing the cuts, but in the integration region defined by H1 (full line) and with a power-law fit (dashed line). Note that the 15% contribution due to double diffraction has been subtracted from data [18].

The Proton Diffractive Structure Functions $F_2^D(\beta, Q^2)$, $F_2^D(x, Q^2)$

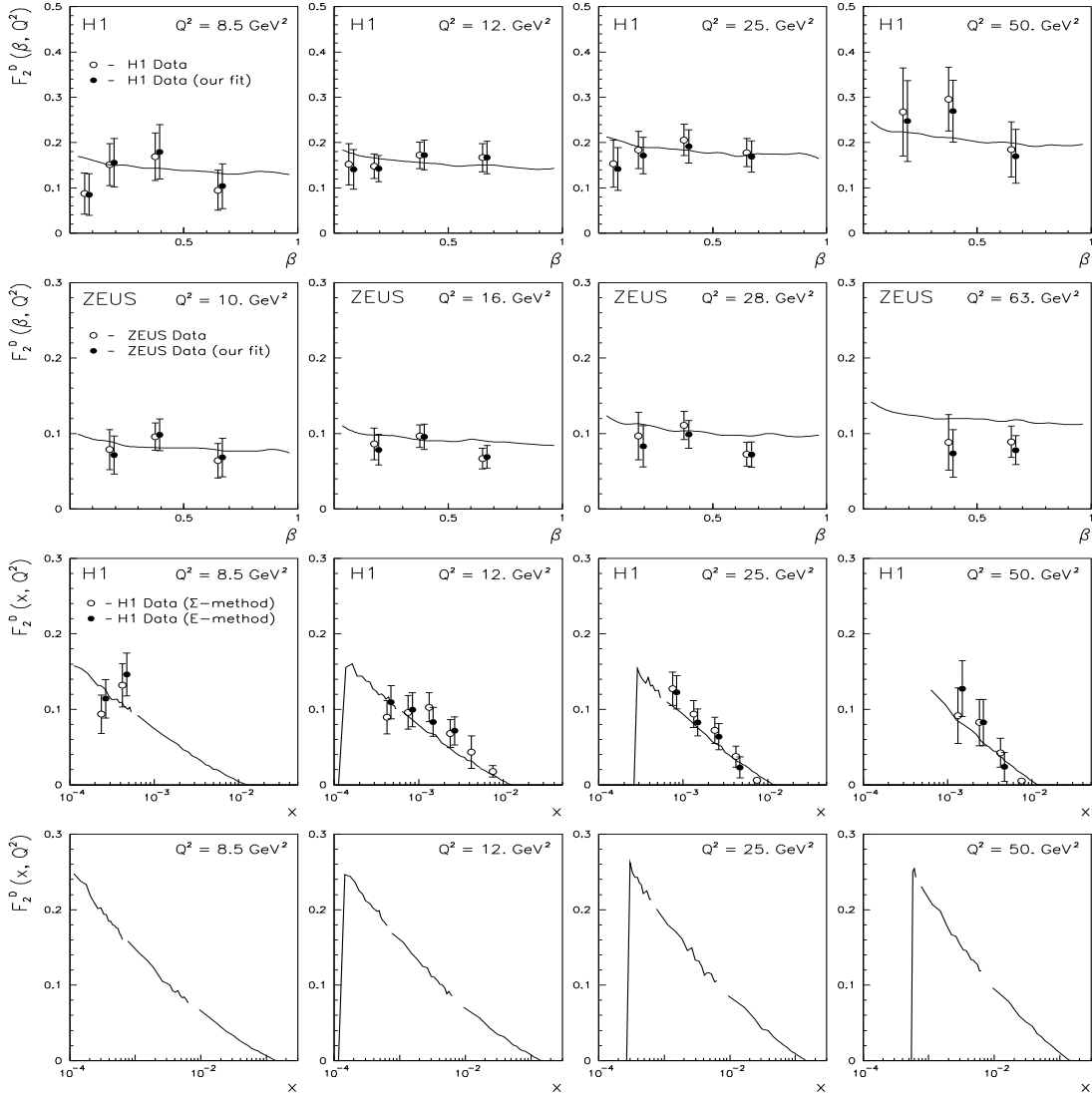


Figure 5: The double differential structure function F_2^D of ZEUS and H1 in terms of β and x_{Bj} , predicted by the model (full line) and compared with the experimental data. The black points on β -distribution correspond to $\alpha_P(0) = 1.069$, obtained in our power-law fit to combined set of HERA data. The black and white points on x_{Bj} -distribution are observations using two different analysis methods [21], the vertical lines are pure kinematic cuts. Note that the 15% contribution due to double diffraction has been subtracted from data [18]. The last four pictures show the expected contribution of single diffraction dissociation, integrated with the relaxed upper limit on η_P (see text above).